

Cationic Nanogel-mediated Runx2 and Osterix siRNA Delivery Decreases Mineralization in MC3T3 Cells

Arun R. Shrivats PhD, Eric Hsu PhD, Saadyah Averick PhD, Molly Klimak, April C. S. Watt MS, Marlene DeMaio MD, Krzysztof Matyjaszewski PhD, Jeffrey O. Hollinger DDS, PhD

Received: 28 August 2014 / Accepted: 17 November 2014 / Published online: 2 December 2014
© The Association of Bone and Joint Surgeons® 2014

Abstract

Background Heterotopic ossification (HO) may occur after musculoskeletal trauma, traumatic brain injury, and total joint arthroplasty. As such, HO is a compelling clinical concern in both military and civilian medicine. A possible etiology of HO involves dysregulated signals in the bone morphogenetic protein osteogenic cascade. Contemporary treatment options for HO (ie, nonsteroidal antiinflammatory drugs and radiation therapy) have adverse effects associated with their use and are not

biologically engineered to abrogate the molecular mechanisms that govern osteogenic differentiation.

Questions/purposes We hypothesized that (1) nanogel-mediated short interfering RNA (siRNA) delivery against Runt-related transcription factor 2 (*Runx2*) and osterix (*Osx*) genes will decrease messenger RNA expression; (2) inhibit activity of the osteogenic marker alkaline phosphatase (ALP); and (3) inhibit hydroxyapatite (HA) deposition in osteoblast cell cultures.

Methods Nanogel nanostructured polymers delivered siRNA in 48-hour treatment cycles against master osteogenic regulators, *Runx2* and *Osx*, in murine calvarial preosteoblasts (MC3T3-E1.4) stimulated for osteogenic differentiation by recombinant human bone morphogenetic protein (rhBMP-2). The efficacy of RNA interference (RNAi) therapeutics was determined by quantitation of messenger RNA knockdown (by quantitative reverse transcription-polymerase chain reaction), downstream protein knockdown (determined ALP enzymatic activity assay), and HA deposition (determined by OsteoImage™ assay).

Results Gene expression assays demonstrated that nanogel-based RNAi treatments at 1:1 and 5:1 nanogel:short interfering RNA weight ratios reduced *Runx2* expression by 48.59% ± 19.53% ($p < 0.001$) and 43.22% ± 18.01% (both $p < 0.001$). The same 1:1 and 5:1 treatments against both *Runx2* and *Osx* reduced expression of *Osx* by 51.65% ± 10.85% and 47.65% ± 9.80% (both $p < 0.001$). Moreover, repeated 48-hour RNAi treatment cycles against *Runx2* and *Osx* rhBMP-2 administration reduced ALP activity after 4 and 7 days. ALP reductions after 4 days in culture by nanogel 5:1 and 10:1 RNAi treatments were 32.4% ± 12.0% and 33.6% ± 13.8% (both $p < 0.001$). After 7 days in culture, nanogel 1:1 and 5:1 RNAi treatments produced 35.9% ± 14.0% and 47.7% ± 3.2% reductions in ALP activity. Osteoblast mineralization data after 21 days suggested that

Two of the authors (ARS, EH) contributed equally.

All institutions in this study, during the study period, received funding from DoD Grant W81XWH1120073, which was awarded by the Defense Medical Research and Development Program, and DMR09-69301.

All ICMJE Conflict of Interest Forms for authors and *Clinical Orthopaedics and Related Research*® editors and board members are on file with the publication and can be viewed on request.

Clinical Orthopaedics and Related Research® neither advocates nor endorses the use of any treatment, drug, or device. Readers are encouraged to always seek additional information, including FDA-approval status, of any drug or device prior to clinical use.

A. R. Shrivats, E. Hsu, M. Klimak, A. C. S. Watt,
J. O. Hollinger (✉)

Department of Biomedical Engineering, Carnegie Mellon University, 700 Technology Drive, Pittsburgh, PA 15219, USA
e-mail: hollinge@cs.cmu.edu; hollinge@andrew.cmu.edu

S. Averick, K. Matyjaszewski
Department of Chemistry, Carnegie Mellon University, 4400 Fifth Ave, Pittsburgh, PA 15213, USA

M. DeMaio
Department of Orthopaedic Surgery, Naval Medical Center Portsmouth, 620 John Paul Jones Cir, Portsmouth, VA 23708, USA

nanogel 1:1, 5:1, and 10:1 RNAi treatments decreased mineralization (ie, HA deposition) from cultures treated only with rhBMP-2 ($p < 0.001$). However, despite RNAi attack on *Runx2* and *Osx*, HA deposition levels remained greater than non-rhBMP-2-treated cell cultures.

Conclusions Although mRNA and protein knockdown were confirmed as a result of RNAi treatments against *Runx2* and *Osx*, complete elimination of mineralization processes was not achieved. RNAi targeting mid- and late-stage osteoblast differentiation markers such as ALP, osteocalcin, osteopontin, and bone sialoprotein may produce the desired RNAi-nanogel nanostructured polymer HO prophylaxis.

Clinical Relevance Successful HO prophylaxis should target and silence osteogenic markers critical for heterotopic bone formation processes. The identification of such markers, beyond RUNX2 and OSX, may enhance the effectiveness of RNAi prophylaxes for HO.

Introduction

Heterotopic ossification (HO) may occur as a consequence of musculoskeletal trauma from blast and high-energy injuries [2, 21, 40, 52], total joint arthroplasty (TJA) [1], traumatic brain injury [17], or spinal cord injury [4, 33, 55, 61]. The incidence rate for HO varies from 15% to 90%, depending on the source of trauma and the grading criteria used [1, 7, 39, 43, 51]. Current treatments for patients with HO emphasize reducing inflammation and/or inactivating tissue-resident stem cells at the trauma site to minimize pathological bone formation. These treatments options include nonsteroidal antiinflammatory drugs (NSAIDs) and radiotherapy (often in combination), although adverse effects have been associated with their use [8, 9, 20, 57]. Surgical excision of HO is another therapeutic option, although recurrence of HO at the surgical site may ensue [10, 13, 65]. Furthermore, contemporary treatment options are not engineered specifically to impede the biological mechanisms responsible for the production of bone in soft tissue. We seek to design a therapeutic that may overcome the limitations of the current generation of treatments and prophylaxes for HO.

In designing a prophylaxis for HO, we emphasized interference with a potent pathway for bone formation and regeneration—the bone morphogenetic protein (BMP)-induced osteogenic signaling cascade. Dysregulation of BMP signaling stimulates osteogenic lineage progression of striated muscle mesenchymal stem cells [14, 56]. Furthermore, a possible HO mechanism may include the inflammatory factor cyclooxygenase-2 (COX-2) and the canonical BMP-based bone-forming pathways [41, 58]. COX-2 expression stimulates prostaglandin E2 (PGE-2) expression in osteoblasts [3, 27]; the PGE-2 and BMP signaling pathways converge at the transcription factor

runx-related protein 2 (RUNX2) [37, 38]. RUNX2 and osteix (OSX) are master regulators of osteogenesis and promote expression of alkaline phosphatase (ALP), osteocalcin (OCN), osteopontin (OPN), and osteonectin (ON) [11, 22, 54]. These molecular cues promote the osteogenic cascade and clinical manifestation of HO.

Therefore, we postulated that silencing *Runx2* and *Osx* expression may be a compelling strategy to prevent osteogenic differentiation and potentially, trauma-induced HO. Furthermore, silencing key molecular factors may be accomplished by ribonucleic acid interference (RNAi) mediated by nonviral vectors [19, 24, 34, 42]. Key intermediaries in the RNAi process are short interfering RNAs (siRNA), which facilitate posttranscriptional silencing of target genes. We previously reported that nanostructured polymers (NSPs) are safe and efficient carriers for the delivery of siRNA in mammalian cell cultures and mouse models [29].

In our current study, we hypothesized that (1) nanogel-mediated siRNA delivery against *Runx2* and *Osx* genes will decrease messenger RNA (mRNA) expression; (2) inhibit activity of the osteogenic marker ALP; and (3) inhibit hydroxyapatite (HA) deposition in osteoblast cell cultures.

Materials and Methods

Nanogel Synthesis

Cationic nanogels were prepared by activators generated by electron transfer atom transfer radical polymerization [5, 35, 36, 45–49, 64] in inverse miniemulsion by copolymerizing quaternized dimethyl aminoethylmethacrylate, oligo(ethylene oxide) methacrylate ($M_n = 300$), and a water-soluble disulfide methacrylate crosslinker with a poly(ethylene glycol 2-bromoisobutyrate) initiator and a copper bromide tris(2-[dimethylamino]ethyl)amine catalyst system dissolved in water. The inverse miniemulsion was prepared by ultrasonication of the aqueous phase in a cyclohexane Span80 solution. After the reaction mixture was degassed, an ascorbic acid solution was injected to generate the active catalyst. Fluorescent nanogels were synthesized by addition of rhodamine methacrylate during synthesis. The nanogels were purified using dialysis and characterized using dynamic light scattering and zeta potential analysis. Further details on nanogel synthesis and characterization can be found in Averick et al. [6].

Nanogel Polyplex Preparation

Nanogel NSPs were complexed with siRNA by addition of requisite amounts in nuclease-free water (Life Technologies, Thermo Fisher Scientific Inc, Waltham, MA, USA).

siRNA in solution (stored at -20°C at $200\ \mu\text{M}$) were thawed and added to nanogel NSPs in solution ($25\ \mu\text{g}/\mu\text{L}$) at the desired NSP:siRNA weight ratio and to a dose of $30\ \text{pmol siRNA}/5\ \mu\text{L}$ treatment. Treatments were prepared in bulk and stored at -20°C between uses.

Cell Culture

MC3T3-E1.4 murine calvarial preosteoblasts were acquired from American Type Culture Collection (Manassas, VA, USA). Cells (initially deep frozen) were thawed in a 37°C water bath. Basal α -minimum essential media (αMEM) was supplemented with 10% heat-inactivated fetal bovine serum and 1% penicillin/streptomycin to formulate complete αMEM . The preosteoblasts were cultured in complete αMEM at 37°C and 5% CO_2 . Cells were passaged using 0.25% trypsin-ethylenediaminetetraacetic acid (EDTA) once they had achieved 70% to 80% confluency and reseeded at a 1:8 subcultivation ratio.

Nanogel Internalization

The siRNA delivery capabilities of nanogel NSPs were validated visually by fluorescently tagging components of our RNAi therapeutics. MC3T3 cells were seeded at a density of 25,000 cells/mL on glass coverslips in 12-well cell-culture plates (each treatment group was performed in triplicate, $N = 3$). Rhodamine nanogels were prepared and delivered to the MC3T3 cells at concentrations of $200\ \mu\text{g}/\text{mL}$. To visually confirm the delivery of a siRNA payload, cyanine 3 (Cy3)-labeled siRNA were complexed with nonfluorescent nanogels at a 1:1 nanogel:siRNA weight ratio and delivered to cells (siRNA dose: $20\ \text{nmol}$). Cells were rinsed with $1 \times$ phosphate-buffered saline (PBS) after 4 hours and fixed with 4% paraformaldehyde with Triton-X 100. Alexa Fluor 633 Phalloidin and DAPI stains were used to visualize the actin cytoskeleton and nuclei, respectively. Cells mounted in Prolong[®] Gold Antifade Reagent (Life Technologies, Thermo Fisher Scientific Inc, Waltham, MA, USA) were imaged at $\times 63$ in oil under a Zeiss LSM 700 laser scanning confocal microscope (Carl Zeiss Microscopy GmbH, Jena, Germany).

Runx2 and *Osx* Gene Expression

The CellsDirect[™] One-Step qRT-PCR Kit with ROX (Life Technologies, Thermo Fisher Scientific Inc, Catalog No. 11754) and an ABI Prism 7000 Sequence Detection System (Applied Biosystems, Foster City, CA, USA) were used for the analysis of *Runx2* and *Osx* mRNA expression in MC3T3

cells. MC3T3 cells were plated at 25,000 cells/mL in 96-well plates at 0.2 mL per well. *Runx2* (Catalog No. 4390771) and *Osx* (Catalog No. 4390771) Silencer Select siRNAs were acquired from Life Technologies (Waltham, MA, USA). siRNA against *Runx2* were delivered at 0 hours; siRNA against *Osx* were delivered at 24 hours along with recombinant human bone morphogenetic protein-2 (rhBMP-2) stimuli at a concentration of $100\ \text{ng}/\text{mL}$. This protocol for osteogenic differentiation and knockdown of *Runx2* and *Osx* was previously validated in MC3T3 cultures [29]. Nanogel:siRNA ratios of 1:1 (NG1) and 5:1 (NG5) were used for siRNA delivery. Lipofectamine[®] RNAiMAX (Life Technologies, Thermo Fisher Scientific Inc, Catalog No. 13778) (abbreviated as LRM) was used as a positive control for siRNA delivery. Target gene expression was evaluated 48 hours after *Osx* siRNA and rhBMP-2 delivery. Cell lysis, RNA extraction, and complementary DNA (cDNA) preparation were carried out according to the CellsDirect One-Step qRT-PCR Kit protocol. Briefly, each reaction contained SuperScript III RT/Platinum *Taq* Mix, $2 \times$ Reaction Mix with ROX, Taqman Gene Expression Assay predesigned primers, and $4\ \mu\text{L}$ of processed cell lysates. Expression of *Runx2* and *Osx* were normalized to *Actb* expression using the comparative C_T method. Fold change data were represented as a percent (normalized to rhBMP-2-treated groups) and were reported as mean \pm SD with $n = 8$ (number of culture wells per treatment).

Alkaline Phosphatase Activity and Cell Viability

Silencing *Runx2* and *Osx* through the osteogenic signaling cascade was evaluated by quantifying ALP activity. To extend assay duration beyond 48 hours of rhBMP-2 delivery, experimental groups received RNAi treatments in a repeated 48-hour cycle with *Runx2* siRNA delivery occurring at 0 hours and *Osx* siRNA + rhBMP-2 delivery ($100\ \text{ng}/\text{mL}$) occurring at 24 hours. Forty-eight-hour treatment cycles were repeated over the course of 4 and 7 days with nanogel NSPs delivering siRNA at 1:1 (NG1), 5:1 (NG5), and 10:1 (NG10) ratios. In 4-day studies, 5:1 and 10:1 NSP:siRNA ratios were evaluated. In 7-day studies, based on the statistically equivalent performance of NG5 and NG10 treatments at 4 days, 1:1 and 5:1 ratios were examined. All groups (except negative controls) received rhBMP-2. Furthermore, scrambled siRNA sequences were delivered as a control to reveal nonspecific gene silencing. Lipofectamine RNAiMAX was used as a positive control for siRNA delivery, defining the positive control as a treatment producing an expected reduction of ALP activity. ALP activity was assessed as previously detailed [63]. Briefly, at experimental endpoints, cells were rinsed with $1 \times$ PBS and lysed with $1 \times$ cell lysis buffer. For cell viability, $100\ \mu\text{L}$

cell lysate were added to a 100 µL solution of Quant-iT™ PicoGreen® dye (1:200 dilution) (Life Technologies, Thermo Fisher Scientific Inc, Waltham, MA, USA). After 2 minutes, DNA content was measured by fluorescence at 490 nm excitation and 535-nm emission wavelengths using a Tecan SpectraFluor (Tecan, Maennedorf, Switzerland). Data were normalized to rhBMP-2-treated groups and expressed as mean ± SD (n = 5). Samples for ALP activity were incubated with p-nitrophenol phosphate (Sigma-Aldrich, St. Louis, MO, USA, Catalog No. N2770), which is dephosphorylated by ALP to produce a colorimetric change detectable by absorbance at 405 nm. P-nitrophenol standards (Sigma-Aldrich, Catalog No. N7660) were used to produce standard curves. Data were normalized to DNA content (by PicoGreen®) and reported as mean ± SD (n = 5) with two technical repeats.

Mineralization in Osteoblast Cultures

The quantitation of HA deposition was performed at 7, 14, and 21 days in MC3T3 cultures by the OsteoImage™ assay (Lonza, Basel, Switzerland, Catalog No. PA-1503). MC3T3 cells were seeded at 25,000 cells/mL in black, 96-well culture plates. Nanogel:siRNA complexes were prepared with both *Runx2* and *Osx* siRNA at 1:1, 5:1, and 10:1 ratios. Specific groups were treated with 48-hour cycles of RNAi treatments against *Runx2* and *Osx* (previously described). Lipofectamine RNAiMAX was used as a control for siRNA delivery. Osteogenic differentiation was induced by delivery of rhBMP-2 (100 ng/mL), and cultures were carried out for 7, 14, and 21 days. The OsteoImage™ (Lonza) assay was carried out per the manufacturer's protocol. Briefly, cells were fixed in 70% ethanol for 20 minutes at room temperature, rinsed with 1 × PBS, and rinsed twice with the wash buffer provided. Samples were stained with diluted staining solution and incubated at room temperature for 30 minutes under protection from light. After incubation, cells were rinsed with wash buffer and measurements were taken at 492 nm excitation and 520-nm emission wavelengths using a Tecan SpectraFluor plate reader. Data were reported as relative fluorescence units (scales linearly with fluorescence) normalized to rhBMP-2-treated groups and expressed as mean ± SD. At each temporal period (7, 14, and 21 days), there were six treatment groups, each with four samples (n = 4), and three measurements per sample.

Statistical Analyses

Data are expressed as arithmetic means and reported with SDs. Sample replicates (n) represent the number of wells

per treatment and are as indicated. Statistical significance was determined by analysis of variance with Tukey's test post hoc analysis for multiple comparisons using Graphpad Prism 6 (La Jolla, CA, USA). Statistical significance is reported as indicated.

Results

Rhodamine-conjugated nanogel NSPs delivered to MC3T3 cells produced strong cytoplasmic fluorescence, indicative of cellular internalization (Fig. 1). Nanogel NSPs complexed with Cy3-conjugated siRNA also produced intracellular fluorescence under Cy3 wavelengths. Untreated cultures did not exhibit any fluorescent signals under rhodamine or Cy3 wavelengths, thus confirming the siRNA delivery capabilities of nanogel NSPs.

Nanogel-based RNAi treatments at 1:1 and 5:1 NSP:siRNA weight ratios reduced *Runx2* and *Osx* mRNA expression in MC3T3 cells (Fig. 2). NG1 (5:1 NSP:siRNA ratio) and NG5 (5:1 NSP:siRNA ratio) delivery of *Runx2* siRNA produced *Runx2* mRNA knockdown of 48.59% ± 19.53% and 43.22% ± 18.01% (p < 0.001, for both). Delivery of both *Runx2* and *Osx* siRNA by nanogel 1:1 and 5:1 carriers produced 56.06% ± 16.57% and 35.27% ± 18.38% reductions (p < 0.001 and p = 0.007, respectively). The relative efficacy of NG1 and NG5 treatments cannot be concluded (*Runx2* siRNA: p > 0.999; *Runx2* + *Osx* siRNA: p = 0.4159). Lipofectamine RNAiMAX treatments delivering *Runx2* and *Runx2* + *Osx* siRNA produced 57.52% ± 16.92% and 54.78% ± 13.90% *Runx2* knockdown, respectively (p < 0.001 for both). There were no differences in *Runx2* mRNA expression between Lipofectamine and nanogel groups when delivering *Runx2* and *Runx2* + *Osx* siRNA (all p > 0.512). Data suggest that nanogel-mediated *Runx2* siRNA delivery produced modest reductions in *Osx* gene expression of 32.6% ± 21.45% and 33.2% ± 14.20% for NG1 and NG5 treatments, respectively (NG1: p = 0.077; NG5: p = 0.0038; Fig. 2B). These treatments, however, did not reduce *Osx* expression to baseline levels indicated by untreated cells (NG1: p = 0.019; NG5: p = 0.023). Nanogel RNAi treatments delivering both *Runx2* + *Osx* siRNA also resulted in reduced *Osx* mRNA expression by 51.65% ± 10.85% and 47.65% ± 9.80% (p < 0.001 for both NG1 and NG5) down to levels consistent with untreated cells (NG1: p = 0.773; NG5: p = 0.517). There were no differences between NG1 and NG5 treatments delivering *Runx2* versus *Runx2* + *Osx* siRNA (NG1: p = 0.750; NG5: p = 0.945). Lipofectamine RNAi treatments produced 43.83% ± 13.58% and 76.43% ± 7.03% reductions in *Osx* mRNA expression when delivering *Runx2* and *Runx2* + *Osx* siRNA, respectively (p < 0.001 for both). Knockdown by Lipofectamine was consistent with baseline *Osx* levels (*Runx2*: p = 0.286; *Runx2* + *Osx*: p > 0.999).

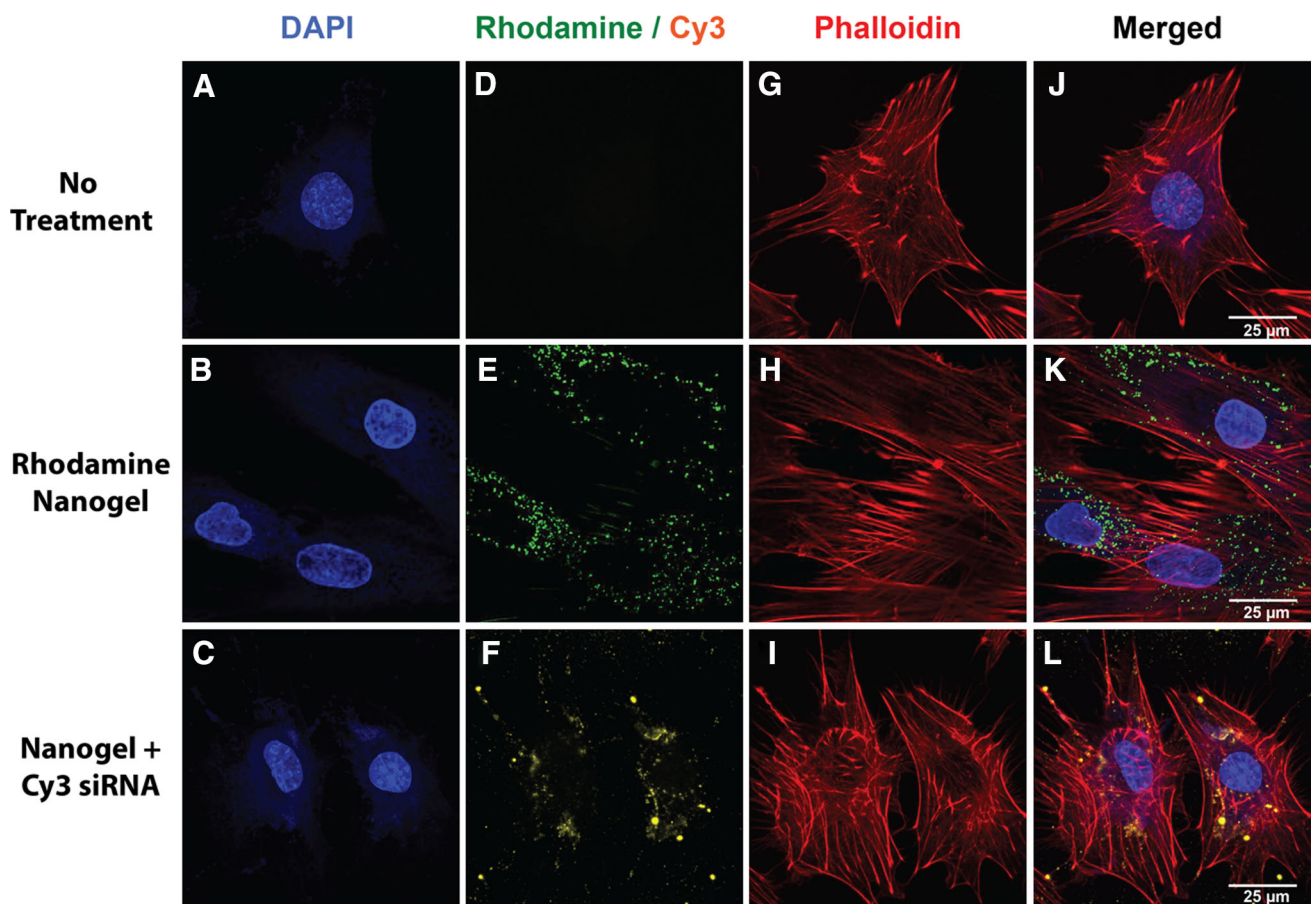


Fig. 1 Internalization of nanogels and polyplexes in MC3T3 cells was verified in confocal images. Top row: Untreated cells demonstrated negligible Cy3 and rhodamine fluorescence (top row). Middle row: Distinct rhodamine signals were detected in samples treated with rhodamine-conjugated nanogels. Bottom row: Cy3-labeled siRNA delivered by nanogel NSP internalized into MC3T3 cells. MC3T3 =

murine calvarial preosteoblast. (A–C) Nuclei of nontreated and treated cells (DAPI, original magnification). (D–F) Fluorescent nanogels and siRNA. (Rhodamine and Cy3, respectively, original magnification). (G–I) F-actin of nontreated and treated cells (Alexa Fluor 633 Phalloidin, original magnification), and (J–L) merged (all channels).

There were no differences between nanogel 1:1 and Lipofectamine treatments delivering *Runx2* + *Osx* ($p = 0.382$).

Nanogel-based RNAi treatments against *Runx2* and *Osx* produced reductions in ALP activity over 4 days without compromising cell viability and proliferation (Fig. 3). Repeated delivery of nanogel polyplexes at 5:1 (NG5) and 10:1 (NG10) NSP:siRNA ratios over 4 days suggested there were no differences in cell viability compared with cells receiving rhBMP treatments measured by DNA content (NG5: $p = 0.967$; NG10: $p > 0.999$). However, Lipofectamine treatments during the same time period reduced DNA content ($p < 0.001$), indicating that Lipofectamine-mediated siRNA delivery may pose cytotoxicity concerns. Evaluation of ALP activity revealed that nanogel 5:1 (NG5) and 10:1 (NG10) treatments reduced ALP expression by $32.4\% \pm 12.0\%$ ($p < 0.001$) and $33.6\% \pm 13.8\%$ ($p < 0.001$), respectively, compared with rhBMP-2-treated controls. As anticipated, the delivery of scrambled (nonspecific) siRNA sequences by

nanogels produced no ALP knockdown in rhBMP-2-treated cells ($p = 0.983$). There were no detected differences between NG5 and NG10 treatments ($p > 0.999$). Overall, nanogel-mediated siRNA treatments (both NG5 and NG10) were comparable to LRM treatments in decreasing ALP activity ($p = 0.618$ and $p = 0.736$, respectively), although without any indications of cytotoxicity or nonspecific silencing. Nanogel RNAi treatments against *Runx2* and *Osx* inhibited ALP activity in rhBMP-2-treated cells over 7 days (Fig. 4). Nanogel 1:1 treatments produced $35.9\% \pm 14.0\%$ reductions in ALP activity ($p < 0.001$) and nanogel 5:1 treatments produced $47.7\% \pm 3.2\%$ knockdown ($p < 0.001$). No differences were determined between NG1 and NG5 treatments ($p = 0.2381$). Lipofectamine treatments of *Runx2* alone and *Runx2* + *Osx* siRNA produced $58.0\% \pm 1.0\%$ and $50.5\% \pm 0.85\%$ ALP knockdown ($p < 0.001$ for both); however, Lipofectamine treatments delivering both *Runx2* and *Osx* siRNA produced $31.1\% \pm 8.5\%$ reductions in cell

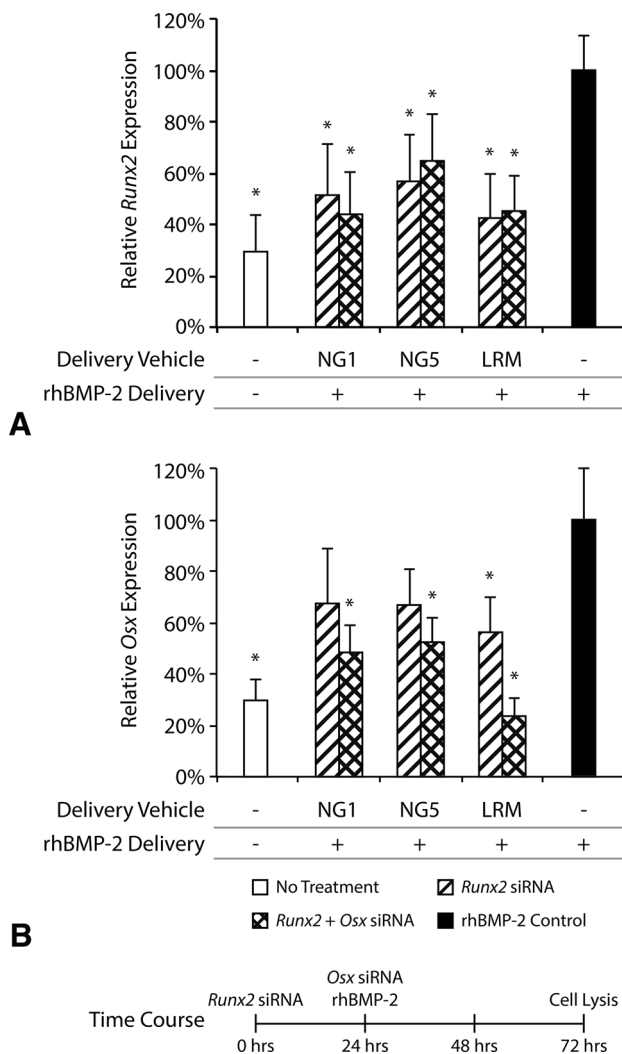


Fig. 2A–B *Runx2* and *Osx* gene expressions in rhBMP-2-treated MC3T3 cells were reduced after delivery of siRNA. **(A)** *Runx2* expression: nanogel-*Runx2* siRNA treatments at 1:1 (NG1) and 5:1 (NG5) NSP:siRNA ratios demonstrated comparable *Runx2* gene silencing as Lipofectamine RNAiMAX (LRM) treatments. The addition of *Osx* siRNA had no impact on *Runx2* expression. **(B)** *Osx* expression: nanogel RNAi treatments against *Runx2* and *Osx* were necessary for *Osx* gene silencing. Asterisks indicate $p < 0.05$ between treatments and rhBMP-2-treated cell cultures. Data reported as mean \pm SD ($n = 8$). MC3T3 = murine calvarial preosteoblast; NG1/NG5 = 1:1/5:1 nanogel:siRNA weight ratios.

viability ($p < 0.001$). In contrast, Lipofectamine delivery of only *Runx2* siRNA reduced cell viability by $4.4\% \pm 6.9\%$ ($p = 0.712$). This, again, suggests that Lipofectamine has a dose-dependent cytotoxic effect triggered by repeated doses. Nanogel-based 1:1 RNAi treatments resulted in $13.6\% \pm 5.8\%$ decreases in cellular content ($p = 0.058$), whereas 5:1 treatments produced $5.3\% \pm 1.8\%$ reductions ($p = 0.920$). Overall, there were no differences between Lipofectamine- and nanogel-mediated *Runx2* + *Osx* siRNA delivery in ALP activity (LRM versus NG1: $p = 0.085$; LRM versus NG5:

$p = 0.998$). Differences in cell viability when delivering *Runx2* and *Osx* siRNA, however, were confirmed (LRM versus NG1: $p = 0.012$; LRM versus NG5: $p < 0.001$).

Nanogel-mediated RNAi treatments produced reductions in HA deposition over 21 days (Fig. 5). Day 7 analyses reflected minimal HA deposition, because mineralization processes typically peak after 2 weeks in culture [28, 60, 68, 70]. Cultures treated with rhBMP-2 exhibited fluorescence levels of 1307.75 ± 36.37 relative fluorescence units (RFUs); untreated cultures produced 1101.50 ± 20.69 RFUs ($p < 0.001$). Cell cultured treated with repeated *Runx2* and *Osx* siRNA dosages at nanogel 1:1, 5:1, and 10:1 ratios produced 1100.75 ± 33.94 , 1108.50 ± 39.37 , and 1084.50 ± 52.16 RFUs (all $p < 0.001$). Cultures receiving Lipofectamine RNAi treatments produced 1096.75 ± 21.20 RFUs ($p < 0.001$). There were no differences among treated cell cultures (all $p > 0.05$), and RNAi-treated cultures exhibited HA deposition levels consistent with untreated cells (all $p > 0.99$). At Day 14, cell culture receiving rhBMP-2 alone exhibited HA levels of 3884 ± 416.5 RFUs. Nanogel 1:1 and 5:1 treatments produced HA levels of 2253 ± 149.8 RFUs ($p < 0.001$) and 2345 ± 203.1 RFUs ($p < 0.001$). Lipofectamine treatments reduced HA levels to 2290 ± 134.2 RFUs ($p < 0.001$). There were no differences between Lipofectamine and nanogel 1:1 and 5:1 treatments ($p > 0.999$ for both). RNAi treatments did not reduce HA deposition to levels comparable to cells untreated by rhBMP-2 (all $p < 0.001$). After 21 days in culture, cells treated with rhBMP-2 produced HA levels of 9590 ± 780.6 RFUs. Nanogel RNAi treatments at 1:1, 5:1, and 10:1 ratios reduced HA levels to 6082 ± 558.0 RFUs ($p < 0.001$), 5615 ± 559.5 RFUs ($p < 0.001$), and 8736 ± 761.5 RFUs ($p = 0.442$), respectively. Lipofectamine RNAi treatments reduced HA deposition to 6592 ± 793.1 RFUs ($p < 0.001$). HA levels for all RNAi treatments were not reduced to baseline levels of cells untreated by rhBMP-2 ($p < 0.001$ for all). There were no differences detected between nanogel 1:1 and 5:1 treatments ($p = 0.902$) and nanogel 1:1 and Lipofectamine treatments ($p = 0.865$). Nanogel-based RNAi treatments against *Runx2* and *Osx* inhibited HA deposition in MC3T3 cell cultures to levels consistent with Lipofectamine RNAiMAX.

Discussion

Current therapies to treat HO (ie, NSAIDs and radiotherapy), if performed early in the HO progression, may successfully modify local microenvironments to be less conducive to heterotopic bone formation. However, these treatments are not biologically engineered to target the molecular mechanisms responsible for bone formation and have notable adverse effects [8, 9, 20, 57]. RNAi, however, may be harnessed to silence master osteogenic factors

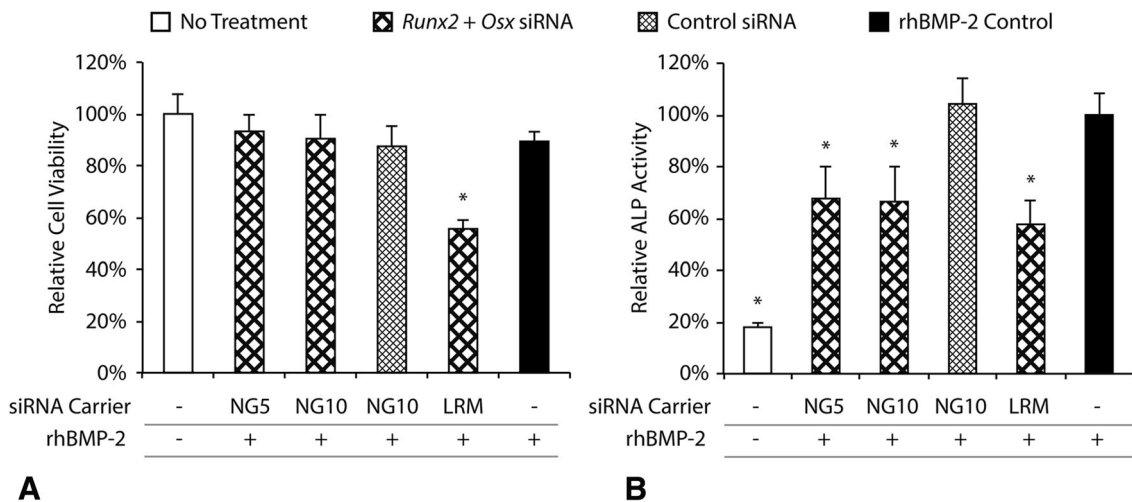


Fig. 3A–B Cell viability and ALP activity of MC3T3 cells were measured after 4 days in culture. **(A)** Cell viability: nanogel treatments did not adversely affect cell viability compared with untreated cells. However, LRM delivery produced cytotoxic effects. **(B)** ALP activity: nanogel:siRNA 5:1 (NG5) and 10:1 (NG10) ratios delivering siRNA against both *Runx2* and *Osx* significantly reduced ALP activity comparable with that of Lipofectamine RNAiMAX

(LRM). Nanogels delivering control (scrambled) siRNA did not significantly impact ALP activity. Asterisks indicate $p < 0.05$ between treatments and rhBMP-2-treated cell cultures. Data reported as mean \pm SD ($n = 5$). MC3T3 = murine calvarial preosteoblast; LRM = Lipofectamine RNAiMAX; NG1/NG5/NG10 = 5:1/10:1 nanogel:siRNA weight ratios.

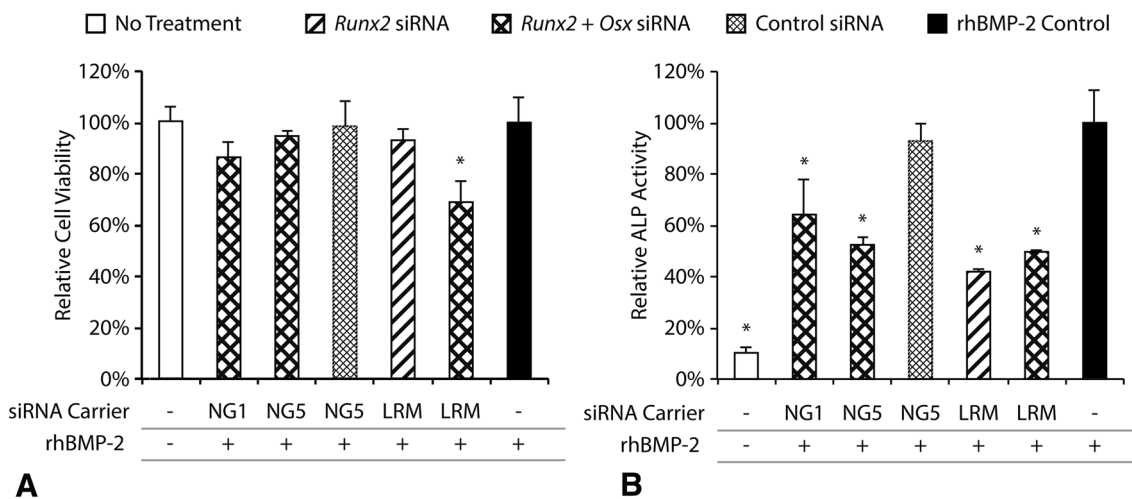


Fig. 4A–B Cell viability and ALP activity in MC3T3 cells were quantitated after 7 days in culture. **(A)** Cell viability: nanogels did not decrease cell viability compared with cells without RNAi treatment. However, Lipofectamine[®] RNAiMAX (LRM) delivering *Runx2* and *Osx* siRNA significantly reduced DNA concentration. **(B)** ALP activity: nanogel:siRNA complexes at 5:1 (NG5) ratios produced

knockdown efficacy consistent with LRM groups. Nanogels delivering control siRNA did not significantly change ALP activity. Asterisks indicate $p < 0.05$ between treatments and rhBMP-2-treated cell cultures. Data reported as mean \pm SD ($n = 5$). MC3T3 = murine calvarial preosteoblast; LRM = Lipofectamine RNAiMAX; NG1/NG5 = 1:1/5:1/10:1 nanogel:siRNA weight ratios.

Runx2 and *Osx* and consequently prevent the aberrant mineralization of muscle tissue without significant off-target effects (ie, HO). Thus, RNAi technology may produce a compelling alternative prophylaxis for HO for administration at trauma sites. We validated the efficacy of cationic nanogels to deliver *Runx2* and *Osx* siRNA and attenuate osteogenic signaling at mRNA and protein levels. We further identified the capability to inhibit HA deposition in osteoblast cell cultures.

A study of this nature, however, is limited by the innate complexity associated with pathological bone formation mechanisms. The intertwining pathways linking poly-trauma to inflammation and HO involve complex signaling and regulatory factors. This interactive biology is difficult to reproduce in vitro. The hallmark of this process is BMP activity; it is known and accepted that BMP-2 is the prototypical molecule for osteogenesis [50]. Terminal osteogenic differentiation is promoted by rhBMP-2; thus,

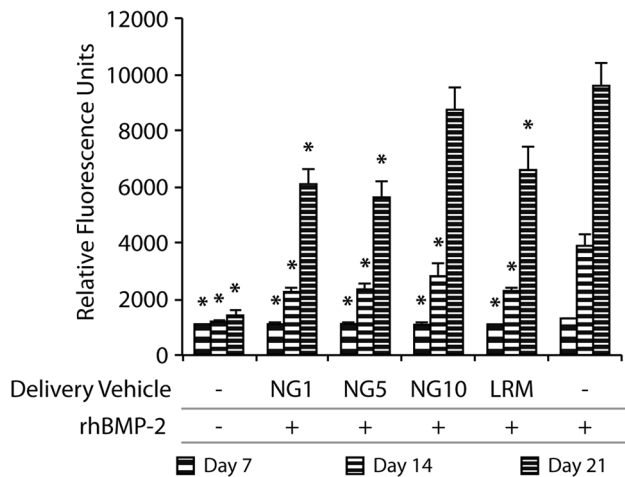


Fig. 5 The OsteoImage™ assay was used to quantitate HA deposition in MC3T3 cells. Nanogel RNAi treatments at 1:1 (NG1) and 5:1 (NG5) ratios significantly reduced HA deposition at 7, 14, and 21 days. This suppressive effect was consistent with Lipofectamine RNAiMAX (LRM) treatments. Nanogel:siRNA complexes at 10:1 ratios (NG10) inhibited HA formation at Days 7 and 14. Asterisks indicate $p < 0.05$ between treatments and rhBMP-2-treated cell cultures. Data reported as mean \pm SD ($n = 4$). MC3T3 = murine calvarial preosteoblast; NG1/NG5/NG10 = 1:1/5:1/10:1 nanogel:siRNA weight ratios; LRM = Lipofectamine RNAiMAX.

abrogating BMP-induced differentiation has a robust biological basis for HO prophylaxis [32, 42].

The knockdown of transient gene expression by RNAi requires calibration to match the temporal expression profiles of the osteogenic cascade. *Runx2* and *Osx* are key transcriptional molecules of the cascade [63]. Thus, dosing, temporal, and spatial parameters of RNAi must be finely tuned. Temporally, *Runx2* and *Osx* expression have been determined to peak within the first 72 hours after BMP stimulation [44]; furthermore, *Runx2* expression is antecedent to *Osx* [69]. Thus, our RNAi treatments were engineered to deliver *Runx2* siRNA 24 hours before and *Osx* siRNA simultaneously to rhBMP-2 administration. Data from our work support the hypothesis that silencing specific genes in the osteogenic cascade may be a compelling prophylaxis for HO. Nanogel-to-siRNA ratios from 1:1 to 10:1 have a significant gene-silencing effect in vitro [29]. Our results suggest decreasing *Osx* gene expression may not affect *Runx2* expression (Fig. 2A). This outcome supports the notion that *Runx2* regulates *Osx* expression and not the reverse [44]. However, *Runx2* siRNA administration by itself did not suppress *Osx* expression; both *Runx2* and *Osx* siRNA were required to produce significant *Osx* gene silencing (Fig. 2B). This suggests *Osx* expression was upregulated through an alternate pathway [12], independent of SMAD protein signaling and *Runx2* activation [31].

RNAi treatment outcomes against *Runx2* and *Osx* suggest a significant inhibitory effect on downstream ALP activity

(Figs. 3B, 4B). The knockdown was determined to be sequence-specific, as evidenced by negligible changes in ALP activity when negative control siRNA polyplexes were delivered (Fig. 4B). Data suggest LRM-mediated siRNA delivery may produce a nonspecific cytotoxic effect. In contrast, nanogel treatments did not significantly affect cell proliferation ($p < 0.05$). Thus, a significant reduction in ALP expression may be attained by NG1 and NG5 RNAi treatments against *Runx2* and *Osx*; however, RNAi treatments did not decrease ALP activity to basal levels of MC3T3 cells not treated with rhBMP-2 ($p < 0.05$). LRM treatments elicited significant reduction in ALP activity, although cytotoxicity issues persisted [18]. Thus, the expression of downstream osteoblast differentiation markers was downregulated as a consequence of RNAi. The reduction of ALP activity may, in turn, prevent late-stage osteoblast maturation, because ALP is known to cleave pyrophosphates that inhibit HA formation and provide the phosphate ions required for HA deposition. To determine if reduction in ALP activity prevented phenotypic cellular change, we analyzed HA deposition in cell cultures.

HA deposition is the hallmark of osteogenic differentiation in MC3T3 cell culture [67]. Silencing *Runx2* and *Osx* over 7, 14, and 21 days produced a significant reduction in HA deposition (Fig. 5). However, reduction of HA deposition to baseline levels was not achieved. Repeated administration of rhBMP-2 (a potent morphogen) over 21 days may have been the cause for this phenomenon. We posit that the repeated delivery of rhBMP-2 challenged the transient efficacy of RNAi therapeutics. To compensate, additional osteogenic signaling factors should be targeted. Mid- and late-stage osteogenic markers including OPN, bone sialoprotein (BSP), and OCN are temporal successors to RUNX2 and OSX expression after rhBMP-2 stimulation [63]. The complex temporal expression profiles of OPN, BSP, and OCN have been elucidated [15, 16, 23, 25, 26, 30, 53, 59, 66]; therefore, a coordinated, temporal RNAi treatment cycle may enhance the duration and intensity of gene silencing and prevent HA deposition in vitro. Consequently, the evolution of RNAi therapeutics must match RNAi targets to their expression profiles. Data suggest that siRNA against *Runx2* and *Osx* should be delivered between Days 0 and 7 and should be succeeded by a permutation of siRNA against *Alp*, *Opn*, *Bsp*, and *Ocn* between Days 7 and 21. This temporal treatment profile is inspired by the biology and physiology of bone formation and key signaling modulators in the osteogenic cascade.

Ultimately, results suggest that silencing *Runx2* and *Osx* may form the basis of an RNAi prophylaxis for HO in the clinic. However, there are notable challenges we must face. During osteogenic differentiation, both RUNX2 and OSX peak within 72 hours of BMP stimulation [44]. A prophylaxis for HO may require delivery before BMP

induction [29]. This treatment schedule, however, may be feasible; the anatomical location of trauma-induced HO is highly predictable [1, 2, 17]. Furthermore, the inflammatory processes preceding bone formation may provide a therapeutic window in which we ultimately deliver HO prophylaxes [62]. These two factors may enable the delivery of a prophylaxis before the maturation of committed osteoblasts at local wound sites.

In conclusion, we report that nanogel-mediated delivery of *Runx2* and *Osx* siRNA inhibits osteoblastic differentiation in murine calvarial preosteoblasts. The nanogel-based siRNA delivery system supports repeated and discrete delivery of therapeutic doses of siRNA without impacting the cellular processes governing viability and proliferation. Knockdown efficacy of nanogels was comparable to LRN treatments without the cytotoxicity of Lipofectamine [18]. By obtaining inspiration from the BMP signaling pathway, we present a biological framework that may prevent HO. However, significant challenges remain: the silencing of mid- and late-stage osteoblast differentiation markers ALP, OPN, BSP, and OCN. Ultimately, the HO prophylactic therapeutic with this biological foundation may eliminate pain and discomfort and improve mobility and quality of life for patients with HO. Further development of this work may produce a compelling clinical contribution to military and civilian medicine.

Acknowledgments We acknowledge the assistance of LTC Krinon Moccia, VC USA and the Animal Care Facility staff at Naval Medical Center Portsmouth, for their valuable collaborative contributions. We also acknowledge the Feinberg Laboratory at Carnegie Mellon University for their assistance in confocal microscopy.

References

- Ahrengart L. Periarticular heterotopic ossification after total hip arthroplasty. Risk factors and consequences. *Clin Orthop Relat Res.* 1991;263:49–58.
- Alfieri KA, Forsberg JA, Potter BK. Blast injuries and heterotopic ossification. *Bone Joint Res.* 2012;1:192–197.
- Arikawa T, Omura K, Morita I. Regulation of bone morphogenetic protein-2 expression by endogenous prostaglandin E2 in human mesenchymal stem cells. *J Cell Physiol.* 2004;200:400–406.
- Aubut JA, Mehta S, Cullen N, Teasell RW, Group E, Scire Research Team. A comparison of heterotopic ossification treatment within the traumatic brain and spinal cord injured population: an evidence based systematic review. *NeuroRehabilitation.* 2011;28:151–160.
- Averick S, Simakova A, Park S, Konkolewicz D, Magenau AJ, Mehl RA, Matyjaszewski K. ATRP under biologically relevant conditions: grafting from a protein. *ACS Macro Letters.* 2011;1:6–10.
- Averick SE, Paredes E, Irastorza A, Shrivats AR, Srinivasan A, Siegwart DJ, Magenau AJ, Cho HY, Hsu E, Averick AA, Kim J, Liu S, Hollinger JO, Das SR, Matyjaszewski K. Preparation of cationic nanogels for nucleic acid delivery. *Biomacromolecules.* 2012;13:3445–3449.
- Bal BS, Lowe JA, A EG, Aletto TJ. Heterotopic ossification after 2-incision total hip arthroplasty. *J Arthroplasty.* 2010;25:538–540.
- Banovac K, Williams JM, Patrick LD, Haniff YM. Prevention of heterotopic ossification after spinal cord injury with indomethacin. *Spinal Cord.* 2001;39:370–374.
- Banovac K, Williams JM, Patrick LD, Levi A. Prevention of heterotopic ossification after spinal cord injury with COX-2 selective inhibitor (rofecoxib). *Spinal Cord.* 2004;42:707–710.
- Brooke MM, Heard DL, de Lateur BJ, Moeller DA, Alquist AD. Heterotopic ossification and peripheral nerve entrapment: early diagnosis and excision. *Arch Phys Med Rehabil.* 1991;72:425–429.
- Celil AB, Campbell PG. BMP-2 and insulin-like growth factor-I mediate Osterix (Osx) expression in human mesenchymal stem cells via the MAPK and protein kinase D signaling pathways. *J Biol Chem.* 2005;280:31353–31359.
- Celil AB, Hollinger JO, Campbell PG. Osx transcriptional regulation is mediated by additional pathways to BMP2/Smad signaling. *J Cell Biochem.* 2005;95:518–528.
- Chalidis B, Stengel D, Giannoudis PV. Early excision and late excision of heterotopic ossification after traumatic brain injury are equivalent: a systematic review of the literature. *J Neurotrauma.* 2007;24:1675–1686.
- Chalmers J, Gray DH, Rush J. Observations on the induction of bone in soft tissues. *J Bone Joint Surg Br.* 1975;57:36–45.
- Chen D, Harris MA, Rossini G, Dunstan CR, Dallas SL, Feng JQ, Mundy GR, Harris SE. Bone morphogenetic protein 2 (BMP-2) enhances BMP-3, BMP-4, and bone cell differentiation marker gene expression during the induction of mineralized bone matrix formation in cultures of fetal rat calvarial osteoblasts. *Calcif Tissue Int.* 1997;60:283–290.
- Cho TJ, Gerstenfeld LC, Einhorn TA. Differential temporal expression of members of the transforming growth factor beta superfamily during murine fracture healing. *J Bone Miner Res.* 2002;17:513–520.
- Dizdar D, Tiftik T, Kara M, Tunc H, Ersoz M, Akkus S. Risk factors for developing heterotopic ossification in patients with traumatic brain injury. *Brain Inj.* 2013;27:807–811.
- Dokka S, Toledo D, Shi X, Castranova V, Rojanasakul Y. Oxygen radical-mediated pulmonary toxicity induced by some cationic liposomes. *Pharm Res.* 2000;17:521–525.
- Dyxhoorn DM, Palliser D, Lieberman J. The silent treatment: siRNAs as small molecule drugs. *Gene Ther.* 2006;13:541–552.
- Farris MK, Chowdhry VK, Lemke S, Kilpatrick M, Lacombe M. Osteosarcoma following single fraction radiation prophylaxis for heterotopic ossification. *Radiat Oncol.* 2012;7:140.
- Forsberg JA, Potter BK. Heterotopic ossification in wartime wounds. *J Surg Orthop Adv.* 2010;19:54–61.
- Gersbach CA, Byers BA, Pavlath GK, Garcia AJ. Runx2/Cbfa1 stimulates transdifferentiation of primary skeletal myoblasts into a mineralizing osteoblastic phenotype. *Exp Cell Res.* 2004;300:406–417.
- Gurkan UA, Gargac J, Akkus O. The sequential production profiles of growth factors and their relations to bone volume in ossifying bone marrow explants. *Tissue Eng A.* 2010;16:2295–2306.
- Hannon GJ, Rossi JJ. Unlocking the potential of the human genome with RNA interference. *Nature.* 2004;431:371–378.
- Hassan MQ, Javed A, Morasso MI, Karlin J, Montecino M, van Wijnen AJ, Stein GS, Stein JL, Lian JB. Dlx3 transcriptional regulation of osteoblast differentiation: temporal recruitment of Msx2, Dlx3, and Dlx5 homeodomain proteins to chromatin of the osteocalcin gene. *Mol Cell Biol.* 2004;24:9248–9261.
- Hassan MQ, Tare RS, Lee SH, Mandeville M, Morasso MI, Javed A, van Wijnen AJ, Stein JL, Stein GS, Lian JB. BMP2

- commitment to the osteogenic lineage involves activation of Runx2 by DLX3 and a homeodomain transcriptional network. *J Biol Chem*. 2006;281:40515–40526.
27. Haversath M, Catelas I, Li X, Tassemeier T, Jager M. PGE(2) and BMP-2 in bone and cartilage metabolism: 2 intertwining pathways. *Can J Physiol Pharmacol*. 2012;90:1434–1445.
 28. Hoemann CD, El-Gabalawy H, McKee MD. In vitro osteogenesis assays: influence of the primary cell source on alkaline phosphatase activity and mineralization. *Pathol Biol (Paris)*. 2009;57:318–323.
 29. Hsu EW, Liu S, Shrivats AR, Watt A, McBride S, Averick SE, Cho HY, Matyjaszewski K, Hollinger JO. Cationic nanostructured polymers for siRNA delivery in murine calvarial pre-osteoblasts. *J Biomed Nanotechnol*. 2014;10:1130–1136.
 30. Huang W, Carlsen B, Rudkin G, Berry M, Ishida K, Yamaguchi DT, Miller TA. Osteopontin is a negative regulator of proliferation and differentiation in MC3T3-E1 pre-osteoblastic cells. *Bone*. 2004;34:799–808.
 31. Javed A, Bae JS, Afzal F, Gutierrez S, Pratap J, Zaidi SK, Lou Y, van Wijnen AJ, Stein JL, Stein GS, Lian JB. Structural coupling of Smad and Runx2 for execution of the BMP2 osteogenic signal. *J Biol Chem*. 2008;283:8412–8422.
 32. Kan L, Kessler JA. Animal models of typical heterotopic ossification. *J Biomed Biotechnol*. 2011;2011:309287.
 33. Kaplan FS, Glaser DL, Hebel N, Shore EM. Heterotopic ossification. *J Am Acad Orthop Surg*. 2004;12:116–125.
 34. Lin L, Chen L, Wang H, Wei X, Fu X, Zhang J, Ma K, Zhou C, Yu C. Adenovirus-mediated transfer of siRNA against Runx2/Cbfa1 inhibits the formation of heterotopic ossification in animal model. *Biochem Biophys Res Commun*. 2006;349:564–572.
 35. Matyjaszewski K. Atom transfer radical polymerization (ATRP): current status and future perspectives. *Macromolecules*. 2012;45:4015–4039.
 36. Matyjaszewski K, Tsarevsky NV. Macromolecular engineering by atom transfer radical polymerization. *J Am Chem Soc*. 2014;136:6513–6533.
 37. McCarthy TL, Chang WZ, Liu Y, Centrella M. Runx2 integrates estrogen activity in osteoblasts. *J Biol Chem*. 2003;278:43121–43129.
 38. McCarthy TL, Ji C, Chen Y, Kim KK, Imagawa M, Ito Y, Centrella M. Runt domain factor (Runx)-dependent effects on CCAAT/enhancer-binding protein delta expression and activity in osteoblasts. *J Biol Chem*. 2000;275:21746–21753.
 39. Medina A, Shankowsky H, Savaryn B, Shukalak B, Tredget EE. Characterization of heterotopic ossification in burn patients. *J Burn Care Res*. 2014;35:251–256.
 40. Melcer T, Belnap B, Walker GJ, Konoske P, Galarneau M. Heterotopic ossification in combat amputees from Afghanistan and Iraq wars: five case histories and results from a small series of patients. *J Rehabil Res Dev*. 2011;48:1–12.
 41. Minghetti L. Cyclooxygenase-2 (COX-2) in inflammatory and degenerative brain diseases. *J Neuropathol Exp Neurol*. 2004;63:901–910.
 42. Mishra S, Vaughn AD, Devore DI, Roth CM. Delivery of siRNA silencing Runx2 using a multifunctional polymer-lipid nanoparticle inhibits osteogenesis in a cell culture model of heterotopic ossification. *Integr Biol (Camb)*. 2012;4:1498–1507.
 43. Nelson ER, Wong VW, Krebsbach PH, Wang SC, Levi B. Heterotopic ossification following burn injury: the role of stem cells. *J Burn Care Res*. 2012;33:463–470.
 44. Nishio Y, Dong Y, Paris M, O'Keefe RJ, Schwarz EM, Drissi H. Runx2-mediated regulation of the zinc finger Osterix/Sp7 gene. *Gene*. 2006;372:62–70.
 45. Oh JK, Bencherif SA, Matyjaszewski K. Atom transfer radical polymerization in inverse miniemulsion: a versatile route toward preparation and functionalization of microgels/nanogels for targeted drug delivery applications. *Polymer*. 2009;50:4407–4423.
 46. Oh JK, Drumright R, Siegwart DJ, Matyjaszewski K. The development of microgels/nanogels for drug delivery applications. *Prog Polym Sci*. 2008;33:448–477.
 47. Oh JK, Siegwart DJ, Lee HI, Sherwood G, Peteanu L, Hollinger JO, Kataoka K, Matyjaszewski K. Biodegradable nanogels prepared by atom transfer radical polymerization as potential drug delivery carriers: synthesis, biodegradation, in vitro release, and bioconjugation. *J Am Chem Soc*. 2007;129:5939–5945.
 48. Oh JK, Siegwart DJ, Matyjaszewski K. Synthesis and biodegradation of nanogels as delivery carriers for carbohydrate drugs. *Biomacromolecules*. 2007;8:3326–3331.
 49. Oh JK, Tang C, Gao H, Tsarevsky NV, Matyjaszewski K. Inverse miniemulsion ATRP: a new method for synthesis and functionalization of well-defined water-soluble/cross-linked polymeric particles. *J Am Chem Soc*. 2006;128:5578–5584.
 50. Peng H, Usas A, Olshanski A, Ho AM, Gearhart B, Cooper GM, Huard J. VEGF improves, whereas sFlt1 inhibits, BMP2-induced bone formation and bone healing through modulation of angiogenesis. *J Bone Miner Res*. 2005;20:2017–2027.
 51. Potter BK, Burns TC, Lacap AP, Granville RR, Gajewski D. Heterotopic ossification in the residual limbs of traumatic and combat-related amputees. *J Am Acad Orthop Surg*. 2006;14:S191–197.
 52. Potter BK, Burns TC, Lacap AP, Granville RR, Gajewski DA. Heterotopic ossification following traumatic and combat-related amputations. Prevalence, risk factors, and preliminary results of excision. *J Bone Joint Surg Am*. 2007;89:476–486.
 53. Prince M, Banerjee C, Javed A, Green J, Lian JB, Stein GS, Bodine PV, Komm BS. Expression and regulation of Runx2/Cbfa1 and osteoblast phenotypic markers during the growth and differentiation of human osteoblasts. *J Cell Biochem*. 2001;80:424–440.
 54. Ryoo HM, Lee MH, Kim YJ. Critical molecular switches involved in BMP-2-induced osteogenic differentiation of mesenchymal cells. *Gene*. 2006;366:51–57.
 55. Sakellariou VI, Grigoriou E, Mavrogenis AF, Soucacos PN, Papatelopoulos PJ. Heterotopic ossification following traumatic brain injury and spinal cord injury: insight into the etiology and pathophysiology. *J Musculoskelet Neuronal Interact*. 2012;12:230–240.
 56. Schmitt JM, Hwang K, Winn SR, Hollinger JO. Bone morphogenetic proteins: an update on basic biology and clinical relevance. *J Orthop Res*. 1999;17:269–278.
 57. Seegenschmiedt MH, Makoski HB, Micke O, German Cooperative Group on Radiotherapy for Benign Disease. Radiation prophylaxis for heterotopic ossification about the hip joint—a multicenter study. *Int J Radiat Oncol Biol Phys*. 2001;51:756–765.
 58. Seibert K, Zhang Y, Leahy K, Hauser S, Masferrer J, Perkins W, Lee L, Isakson P. Pharmacological and biochemical demonstration of the role of cyclooxygenase 2 in inflammation and pain. *Proc Natl Acad Sci U S A*. 1994;91:12013–12017.
 59. Shea CM, Edgar CM, Einhorn TA, Gerstenfeld LC. BMP treatment of C3H10T1/2 mesenchymal stem cells induces both chondrogenesis and osteogenesis. *J Cell Biochem*. 2003;90:1112–1127.
 60. Shea LD, Wang D, Franceschi RT, Mooney DJ. Engineered bone development from a pre-osteoblast cell line on three-dimensional scaffolds. *Tissue Eng*. 2000;6:605–617.
 61. Shehab D, Elgazzar AH, Collier BD. Heterotopic ossification. *J Nucl Med*. 2002;43:346–353.
 62. Shrivats AR, Alvarez P, Schutte L, Hollinger JO. Bone regeneration. In: Lanza R, Langer R, Vacanti J, eds. *Principles of Tissue Engineering*. San Diego, CA, USA: Elsevier; 2014:1201–1221.

63. Shrivats AR, Hollinger JO. The delivery and evaluation of RNAi therapeutics for heterotopic ossification pathologies. In: Turksen K, Vunjak-Novakovic G, eds. *Biomimetics and Stem Cells: Methods and Protocols*. New York, NY, USA: SpringerLink; 2013.
64. Simakova A, Averick SE, Konkolewicz D, Matyjaszewski K. Aqueous ARGET ATRP. *Macromolecules*. 2012;45:6371–6379.
65. Tsionos I, Leclercq C, Rochet JM. Heterotopic ossification of the elbow in patients with burns. Results after early excision. *J Bone Joint Surg Br*. 2004;86:396–403.
66. Ulsamer A, Ortuno MJ, Ruiz S, Susperregui AR, Osses N, Rosa JL, Ventura F. BMP-2 induces Osterix expression through up-regulation of Dlx5 and its phosphorylation by p38. *J Biol Chem*. 2008;283:3816–3826.
67. Wang D, Christensen K, Chawla K, Xiao G, Krebsbach PH, Franceschi RT. Isolation and characterization of MC3T3-E1 preosteoblast subclones with distinct in vitro and in vivo differentiation/mineralization potential. *J Bone Miner Res*. 1999;14:893–903.
68. Wang YH, Liu Y, Maye P, Rowe DW. Examination of mineralized nodule formation in living osteoblastic cultures using fluorescent dyes. *Biotechnol Prog*. 2006;22:1697–1701.
69. Zhang C. Transcriptional regulation of bone formation by the osteoblast-specific transcription factor *Osx*. *J Orthop Surg Res*. 2010;5:37.
70. Zhu B, Bailey SR, Mauli Agrawal C. Calcification of primary human osteoblast cultures under flow conditions using polycaprolactone scaffolds for intravascular applications. *J Tissue Eng Regen Med*. 2011 Sep 20 [Epub ahead of print].